Tailoring nonlinear frequency generation in graded-index multimode fibers

M.A. Eftekhar [1*], Z. Sanjabi Eznaveh [1], J. E. Antonio Lopez[1], M. Kolesik[2], A. Schülzgen[1], F. W. Wise[3], D. N. Christodoulides[1], And R. Amezcua Correa[1]

[1]*CREOL, The College of Optics and Photonics, University of Central Florida, Orlando, Florida 32816, USA*
[2]*College of Optical Sciences, University of Arizona, Tucson, AZ 85721, USA.*
[3]*School of Applied and Engineering Physics, Cornell University, Ithaca, New York 14853, USA.*
m.a.eftekhar@knights.ucf.edu

Abstract: We demonstrate that frequency generation in multimode graded-index fibers can be tailored through appropriate fiber design. This is achieved by exploiting a geometric parametric instability which can be utilized for developing novel fiber light sources.

OCIS codes: :(190.4370) Nonlinear optics, fibers; (190.4410) Nonlinear optics, parametric processes; (190.4380) Nonlinear optics, four-wave mixing; (060.0060) Fiber optics and optical communications

1. Introduction

An intense continuous wave (CW) propagating in the anomalous dispersion region of an optical fiber is known to undergo modulation instability (MI). During this process, the CW background breaks up into a train of optical solitons, resulting from the amplification of noise spectral sidebands [1]. Modulation instability can also take place in the normal dispersive regime because of cross-phase modulation [2], or in systems with periodic variations in either dispersion [3] or gain [4]. While in single-mode optical fibers, MI manifests itself purely as a temporal effect, in multimode fibers this same mechanism is considerably more involved due to the additional spatial degrees of freedom [5].

Quite recently, there has been a growing interest in multimode fibers (MMFs) for next-generation high-capacity telecommunication systems [6], and high-energy fiber lasers [7]. In light of these investigations, a better understanding of the nonlinear dynamics in MMFs is now imperative. As first shown by Longhi [8], the periodic spatial refocusing of a beam - taking place in a graded-index fiber, can lead to a geometric parametric instability (GPI), regardless of the sign of fiber dispersion. This GPI process has been recently observed in a series of experiments [9,10]. In these studies, this parametric instability was triggered in both the anomalous and normal dispersive region and produced a series of intense frequency peaks in the visible and near-infrared (NIR) spectral range. Moreover, the presence of many interacting modes introduces multiple pathways for phase-matched nonlinear wave-mixing generation. Consequently, a high intensity pump pulse propagating in a graded-index MMF can produce ultra-broadband supercontinuum, beam clean-up, and multimode solitons [5,9–11].

Here, we provide a comprehensive investigation concerning the role of core size scaling on GPI in highly multimode parabolic fibers. The resulting side band generation was studied in detail in a number of fiber structures with diameters ranging from 50 to 80 μm. In all cases, the sideband frequency shift was found to follow a $a^{-1/2}$ relation, with a being the core radius. These results are in good agreement with analytical predictions and numerical simulations carried out using a generalized unidirectional pulse propagation equation (gUPPE) code [12]. Our study can lead to a new class of light sources with a tailored spectral output content.

2. Experiments and simulations

Figure 1 shows a schematic representation of the experimental setup. The single-mode output of an amplified Q-switched micro-chip laser, delivering 95 μJ pulses at 1064 nm, with a pulse duration of 400 ps and a repetition rate of 500 Hz, was coupled into the graded-index MMF samples. The free space coupling efficiency was greater than 85% using a 50 mm focal length lens. A half wave plate and a polarizing beam splitter cube (PBSC) were used to control the input power. The initial spatial launching conditions were adjusted using a three-axis translation stage. A large set of transverse spatial modes was excited by focusing the laser beam on the front facet of the fiber. Light at the output of the graded-index MMF under test was collected by a multimode patch cord (105 μm core diameter) and analyzed using an optical spectrum analyzer (OSA) covering the spectral range from 350 nm to 1750 nm (857.1-171.4 THz). The parabolic multimode fibers used in our experiments were in-house fabricated with core diameters of 50 μm, 60 μm and 80 μm, and had a maximum refractive index contrast of $\sim 16\times10^{-3}$ with respect to the cladding. Figures 2 (a-c), depict a series of rather intense discrete peaks in the visible regime obtained using an optical grating. The pump peak power used was ~185 kW and the fiber length was ~5 m in all the experiments. The

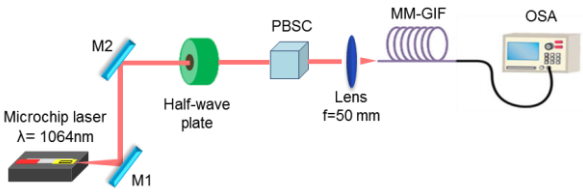

Fig. 1. Schematic representation of the experimental setup. Pulses from a Q-switched microchip laser at 1064 nm are launched into a graded-index MMF.

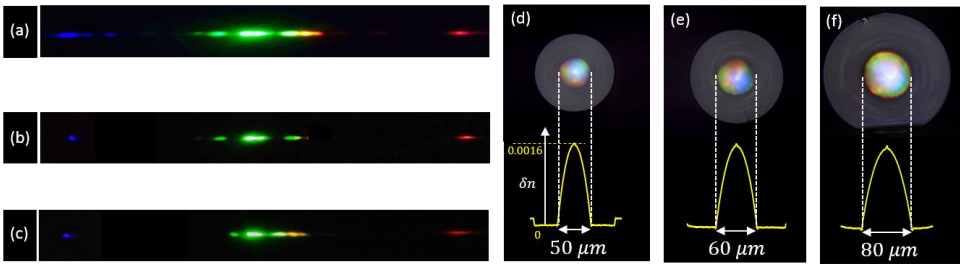

Fig. 2. Images of dispersed visible spectra obtained in a 5m-long graded-index MMF with (a) 50 μm, (b) 60 μm (c) 80 μm core diameter. The peak pump power is 185 kW at 1064 nm. Microscope images of the fabricated fiber samples (d) 50 μm, (e) 60 μm (f) 80 μm along with their corresponding index profiles.

optical microscope images of the fiber cross sections and their corresponding parabolic refractive index profiles as measured using a profilometer are shown in Figs. 2 (d-f). Following the theoretical model of Ref. [12], one can show that the spatiotemporal wave instabilities in nonlinear graded-index MMFs are in agreement with those expected from a Floquet–Bloch theory. The periodic squeezing of light taking place in graded-index multimode fibers incites modulation instability - regardless of the sign of dispersion [8]. Because of this mechanism, the periodic spatial breathing of light leads to energy coupling from the pump to the sidebands having frequencies, $\omega_{SB_m} = \omega_p \pm \sqrt{m}\omega_G$ where $\omega_G{}^2 = 2\delta / \left|k_0^{"}\right|$, and δ stands for the regular spacing between the propagation constants of consecutive modes $\delta = a^{-1}\sqrt{2\Delta}$. Here, $\Delta = (n_{core} - n_{clad})/n_{core}$, and a is the core radius. In the above expression, m is an integer (corresponding to the order of the sidebands) and $k_0^{"}$ is the fiber dispersion coefficient. At 1064 nm where the experiments were performed $k_0^{"} = 1.6427\times10^{-26} m^{-1}s^2$. In all cases, the input spot size of the laser beam was intentionally chosen to be different from that of the Gaussian fundamental mode LP_{01}, so as to simultaneously excite a large set of LP_{0m} modes, necessary to initiate the required periodic spatial compression. Accordingly, from these values, the first sidebands (m=1, in the visible) are expected to be observed at 414.61 THz, 403.05 THz, and 386.83 THz.

To better understand the experimental observations, numerical simulations were carried out based on a general unidirectional pulse propagation equation (gUPPE) approach. In doing so, the spatiotemporal evolution of the total electric field in the presence of linear and nonlinear effects is computed at each step. Unlike conventional beam propagation schemes that typically handle a finite number of modes, the gUPPE approach allows one to simultaneously analyze the evolution of hundreds or thousands of modes (as in our experiments) [12]. Linear (dispersion, guiding) and nonlinear effects (self-phase modulation (SPM), FWM, third harmonic generation, shock and Raman effects) are accounted for in our code. In our simulations, the time window was 6 ps, the size of the spatial window was 70 μm × 70 μm and an adaptive integration step size of 1-2 μm was used. The pulse width was taken to be 400 fs and a beam waist of 27 μm was assumed at the fiber input. In all our calculations the propagation distance was 40 cm. As an example, Fig. 3 (a) illustrates the spectral evolution as a function of propagation distance in the graded-index MMF with a 50 μm core diameter. In this figure the spectral broadening due to SPM can be clearly seen during the early stages of propagation. Subsequently, after ~7 cm, a series of sidebands emerge (extending from NIR to the visible) with the first one located at 724 nm. On the other hand, after 20 cm of propagation, the first GPI induced NIR line at ~2 μm appears. More spectral features eventually emerge as a result of Raman and FWM intermixing. Our simulations indicate that the first sideband is always the most intense compared to the rest. In a similar fashion the two other fiber samples were simulated.

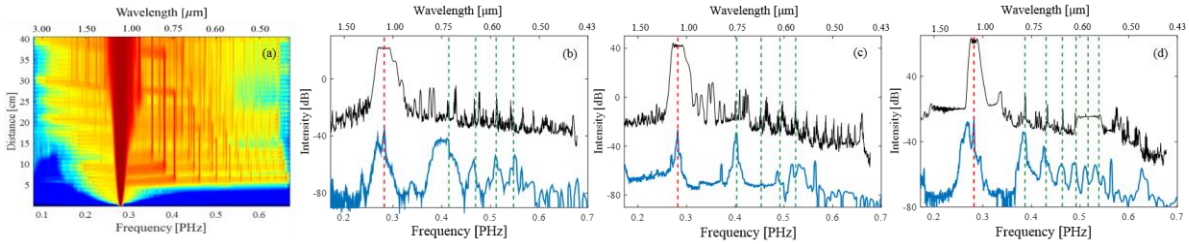

Fig 3. (a) Spectral evolution upon propagation in a 40 cm long graded-index MMF with a 50 μm core diameter, as obtained from gUPPE simulations. Several lines emerge in the visible after a distance of ~7 cm. (b-d) Simulated (black curve) and measured (blue curve) spectra unfolding in a parabolic multimode fiber with a (b) 50 μm , (c) 60 μm (d) 80 μm core diameter. The red dotted lines represent the position of the pump at 1064 nm while the green lines indicate the position of the expected GPI induced sidebands. A redshift in the sidebands proportional to a^{-1} is observed as the core diameter increases.

Figures 3 (b-d) compare the frequency positions of the induced GPI sidebands observed experimentally with those expected from numerical and analytical results for the three fibers under consideration. In this figure, the dashed green lines represent the frequency positions as expected from analytical results. Meanwhile, the black and blue solid curves illustrate the simulated and measured spectra, respectively. This figure indicates that there is an excellent agreement between the experimental observations, numerical simulations and theoretical predictions. In Fig. 3 (b) and (d) corresponding to core diameters of 50 μm and 80 μm, the numerical and experimental results agree well up to 5th sideband. In Fig. 3 (c) the second sideband was not particularly visible. Both theory and simulations predict that for every anti-Stokes GPI sideband, there should be a corresponding Stokes counterpart with an equal frequency detuning from the pump. However, due to the limited operational range of our OSA we were unable to observe the NIR Stokes spectral peaks. Our theoretical analysis indicates that a change in the core diameter from 50 μm to 80 μm, can redshift the position of the first sideband (m=1) by Δf=28 THz (~ 100 nm). For higher order sidebands (m>1), this shift scales according to $\sqrt{m}\Delta f$. These unique nonlinear effects in parabolic-index fibers can be potentially exploited in designing novel light sources with a tailored spectral content. Of interest is to study these processes in tapered multimode fibers to optimize supercontinuum generation with high spectral power densities.

3. Conclusion

We have systematically investigated the impact of fiber core size on the frequency sideband generation induced by ageometric parametric instabilities in a graded-index MMF when pumped in the normal dispersive region. The theoretically expected redshift in the nonlinear GPI frequency generation is experimentally verified in a set of parabolic fibers with increasing diameters. The observed frequency generation can be accurately predicted based on analytical models and numerical simulations.

This work was supported by ONR (MURI N00014-13-1-0649), HEL-JTO and ARO (W911NF- 12-1-0450), AFOSR FA9550-15- 10041.

References

1. A. Hasegawa and W. Brinkman, "Tunable coherent IR and FIR sources utilizing modulational instability," IEEE J. Quantum Electron. **16**, 694–697 (1980).
2. G. P. Agrawal, "Modulation instability induced by cross-phase modulation," Phys. Rev. Lett. **59**, 880–883 (1987).
3. F. Consolandi, C. De Angelis, A.-D. Capobianco, G. Nalesso, and A. Tonello, "Parametric gain in fiber systems with periodic dispersion management," Opt. Commun. **208**, 309–320 (2002).
4. S. M. J. Kelly, "Characteristic sideband instability of periodically amplified average soliton," Electron. Lett. **28**, 806–807 (1992).
5. L. G. Wright, D. N. Christodoulides, and F. W. Wise, "Controllable spatiotemporal nonlinear effects in multimode fibres," Nat. Photonics **9**, 306–310 (2015).
6. D. J. Richardson, J. Nilsson, and W. A. Clarkson, "High power fiber lasers: current status and future perspectives [Invited]," J. Opt. Soc. Am. B **27**, B63 (2010).
7. X. Zhu, A. Schülzgen, H. Li, L. Li, Q. Wang, S. Suzuki, V. L. Temyanko, J. V. Moloney, and N. Peyghambarian, "Single-transverse-mode output from a fiber laser based on multimode interference," Opt. Lett. **33**, 908 (2008).
8. S. Longhi, "Modulational instability and space time dynamics in nonlinear parabolic-index optical fibers," Opt. Lett. **28**, 2363 (2003).
9. K. Krupa, A. Tonello, A. Barthélémy, V. Couderc, B. M. Shalaby, A. Bendahmane, G. Millot, and S. Wabnitz, "Observation of Geometric Parametric Instability Induced by the Periodic Spatial Self-Imaging of Multimode Waves," Phys. Rev. Lett. **116**, 183901 (2016).
10. G. Lopez-Galmiche, Z. Sanjabi Eznaveh, M. A. Eftekhar, J. Antonio Lopez, L. G. Wright, F. Wise, D. Christodoulides, and R. Amezcua Correa, "Visible supercontinuum generation in a graded index multimode fiber pumped at 1064 nm," Opt. Lett. **41**, 2553 (2016).
11. L. G. Wright, W. H. Renninger, D. N. Christodoulides, and F. W. Wise, "Spatiotemporal dynamics of multimode optical solitons," Opt. Express **23**, 3492–3506 (2015).
12. J. Andreasen and M. Kolesik, "Nonlinear propagation of light in structured media: Generalized unidirectional pulse propagation equations," Phys. Rev. E **86**, 36706 (2012).